

## III-F Ultrafast Molecular Dynamics Studied by Time-Resolved Photoelectron Imaging

Femtosecond pump-probe time-resolved photoelectron imaging is a novel experimental approach to probe electronic and nuclear dynamics in real time. Since photoionization can occur from any part of the potential energy surfaces with any multiplicity, the method provides a versatile means to follow dephasing and reaction processes.

### III-F-1 Ionization Dynamics of NO $A(2\Sigma^+)$ State Studied by Time-Resolved Photoelectron Imaging

TSUBOUCHI, Masaaki<sup>1</sup>; SUZUKI, Toshinori  
(<sup>1</sup>GUAS)

Photoionization dynamics of NO from the  $A^2\Sigma^+$  ( $3s\sigma$  Rydberg) state is studied by femtosecond photoelectron imaging method. The photoelectron angular distribution (PAD) observed in the laboratory frame (LF) is convolution of the PAD in the molecular frame (MF) with the molecular axis distribution in space. Our method utilizes a rotational wavepacket created by coherent excitation of the molecular ensemble to control the axis distribution, and the LF-PAD is measured as a function of this distribution. Then, the LF-PAD is deconvoluted with the axis distribution to obtain the MF-PAD. The PADs in (1+1') REMPI *via* the  $A$  state are well expressed by expansion with the Legendre polynomials,

$$I(\theta; t) \propto 1 + \beta_2(t)P_2(\cos\theta) + \beta_4(t)P_4(\cos\theta).$$

Figure 1 shows the time dependence of the expansion coefficients,  $\beta_L$ , observed for several probe wavelengths. All profiles exhibit modulation with 8.4 ps time period in agreement with the rotational constant of NO in the  $A$  state,  $B = 1.997\text{ cm}^{-1}$ . The phase of the modulation varies with the probe wavelength, clearly indicating that the ionization dynamics of NO from the  $A$  state is energy-dependent. The ionization dynamical parameters are extracted from the  $\beta_L$  parameters.

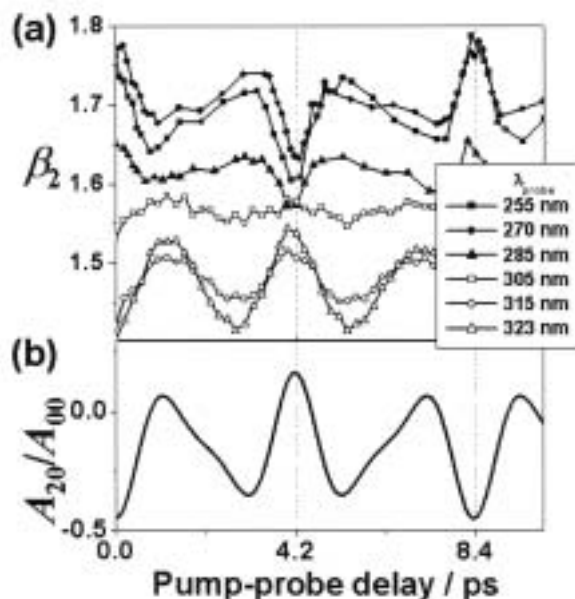


**Figure 1.** (a) Temporal profiles of the  $\beta_2$  anisotropy parameter of LF-PADs observed by [1+1'] femtosecond photoelectron imaging with several probe wavelengths. (b) Calculated time evolution of the alignment parameter,  $A_{20}/A_{00}$ , for the molecular axis distribution,

$$P(\theta, \phi) = A_{00}Y_{00}(\theta, \phi) + A_{20}Y_{20}(\theta, \phi),$$

on the optically excited NO  $A$  state.

### III-F-2 Theoretical Analysis of Rotational Revivals in Intersystem Crossing in Pyrazine

TSUBOUCHI, Masaaki<sup>1</sup>; WHITAKER, Benjamin J.<sup>2</sup>; SUZUKI, Toshinori  
(<sup>1</sup>GUAS; <sup>2</sup>Leeds Univ.)

In our previous work, we have visualized the decay of the  $S_1$  and the buildup of the  $T_1$  state in the  $S_1(n, \pi^*) \rightarrow T_1(n, \pi^*)$  intersystem crossing (ISC) of pyrazine using the (1+2') femtosecond photoelectron imaging.<sup>1,2</sup> A rotational wavepacket motion created by coherent excitation of multiple rovibrational states in the  $S_1$  state was clearly observed in the temporal behavior of photoelectron intensities. The signature of the rotational wavepacket motion is also seen in the  $T_1$  state, however, this amplitude was much smaller than the one observed for the  $S_1$  state. We attempted theoretical analysis of this phenomenon. A model Hamiltonian matrix for a singlet state and multiple triplet states is diagonalized to form molecular eigenstates, and coherent excitation of these ensemble states is considered. The spin-orbit coupling strength and the density of triplet states are assumed to reproduce the observed dephasing time. The time-dependent alignment in the  $S_1$  and  $T_1$  states are calculated. Figure 1 shows the experimental and calculated time evolutions of the alignment parameter,  $A_{20}/A_{00}$ , for the molecular axis distribution,

$$P(\theta, \phi) = A_{00}Y_{00}(\theta, \phi) + A_{20}Y_{20}(\theta, \phi).$$

The rotational quantum beats in the singlet and triplet signals are reproduced well, where the model correctly predicts weaker alignment for the triplet states.

#### References

- 1) T. Suzuki *et al.*, *J. Chem. Phys.* **111**, 4859 (1999).
- 2) Tsubouchi *et al.*, *Phys. Rev. Lett.* **115**, 8810 (2001).

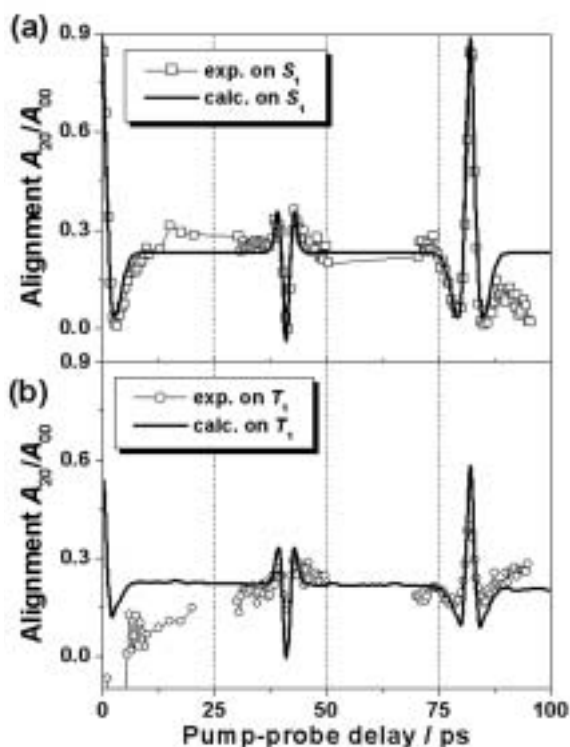


**Figure 1.** Time evolutions of the alignment parameter,  $A_{20}/A_{00}$ , for the molecular axis distribution,

$$P(\theta, \phi) = A_{00}Y_{00}(\theta, \phi) + A_{20}Y_{20}(\theta, \phi),$$

on (a) the  $S_1$  and (b) the  $T_1$  state. Square ( $\square$ ) and circle ( $\circ$ ) represent the experimentally determined alignment parameter which derived from the time profiles of the photoionization partial cross section from the  $S_1$  and the  $T_1$  state, respectively. Solid lines are simulation profiles taking into account the rotational wavepacket motion.

### III-F-3 Femtosecond Photoelectron Imaging on Pyridazine: $S_1$ Decay Rate and $3s$ and $3p$ Rydberg State Energetics

**KIM, Sang Kyu<sup>1</sup>; MATSUMOTO, Yoshiteru;  
SUZUKI, Toshinori**  
(<sup>1</sup>Inha Univ., Korea)

Diazabenzenes have received extensive experimental and theoretical studies as the benchmark systems for investigation of electronic dephasing processes. In particular, pyrazine is the best-studied molecule of an intermediate case and it is well accepted now that the optically prepared  $S_1$  pyrazine dephases into the  $T_1$  manifold with a lifetime of 110 ps. Our previous study on pyrazine by time-resolved photoelectron imaging has firmly established this dynamics by visualizing both the decay of the  $S_1$  and the buildup of  $T_1$  characters in real time.<sup>1)-3)</sup> Comparing with pyrazine and pyrimidine, pyridazine is the least-studied member of diazabenzene. There seem to be still debates on various fundamental properties of excited state such as the  $S_1$  lifetime, spectral assignment of  $S_1$  origin, and energetics of low-lying Rydberg states. Another interesting issue is that although pyrazine dephases mainly to the triplet manifold, it has been suggested that pyridazine dephases down to the ground electronic state. We have performed the first time-resolved study on the excited states of pyridazine by femtosecond photoelectron imaging. The lifetime of the  $S_1$  state is 340 ps at the origin and decreases at higher vibrational energies, and no clear signature of the triplet states was observed. The  $3s$  ( $n^{-1}$ ) and  $3p$  ( $n^{-1}$ ) Rydberg states of pyridazine are identified in angle- and energy-resolved photoelectron images obtained by the  $(1+2')$  excitation where these Rydberg states act as intermediate resonant states in photoionization process, providing respective term values of 5.67 and 6.27 eV.

#### References

- 1) T. Suzuki *et al.*, *J. Chem. Phys.* **111**, 4859 (1999).
- 2) Tsubouchi *et al.*, *Phys. Rev. Lett.* **115**, 8810 (2001).
- 3) Song *et al.*, *J. Chem. Phys.* **86**, 4500 (2001).

## III-G Non-Adiabatic Photodissociation Dynamics of Fundamental Molecules

Detailed investigation on photodissociation dynamics of fundamental molecules is extremely important not only for elucidating chemical reaction mechanisms but also for accurate modeling of atmospheric chemistry. Hyperthermal kinetic energy distribution of reaction products, hot band contribution in photoabsorption, and non-adiabatic dynamics are important for understanding isotope fractionation, branching ratios in bimolecular reactions *etc.* in the atmosphere.

### III-G-1 Non-Adiabatic Bending Dissociation of OCS: The Effect of Bending Excitation on the Transition Probability

**KATAYANAGI, Hideki; SUZUKI, Toshinori**

[*Chem. Phys. Lett.* **360**, 104 (2002)]

In our previous work, an interesting non-adiabatic

dissociation mechanism of OCS induced by fast bending motion in the electronically excited state has been discovered.<sup>1)</sup> In the present work, UV photodissociation dynamics of OCS starting from the bending excited (010) state was compared to that from the ground vibrational state (000). The rotational distribution of  $\text{CO}(X^1\Sigma^+)$  was measured by (2+1) resonance enhanced multiphoton ionization, in which dissociations from the two different initial states were discriminated from the

translational energies of the CO fragments. Quantitative analysis revealed that the non-adiabatic transition probability in dissociation starting from (010) was 0.21 that is similar to but slightly smaller than the value, 0.34, from (000).

#### Reference

1) Suzuki *et al.*, *J. Chem. Phys.* **109**, 5778 (1998).

### III-G-2 Velocity Map Fragment Imaging on 205 nm Photodissociation of Nitrous Oxide

KATAYANAGI, Hideki; NISHIDE, Tatsuhiro;  
SUZUKI, Toshinori

Photodissociation of N<sub>2</sub>O at 205 nm is reexamined by the velocity map ion imaging of N<sub>2</sub> and O(<sup>1</sup>D<sub>2</sub>) fragments. The kinetic energy distribution of the O atoms measured by using (2+1) REMPI via the <sup>1</sup>P<sub>1</sub> state is in excellent agreement with the one reported previously by

a conventional imaging method without two-dimensional space focusing.<sup>1)</sup> The angular distribution of the O atoms is expressed by expansion with up to the 6-th order Legendre polynomial, indicating the orbital alignment as reported previously.<sup>1)</sup> A bell-shaped rotational distribution of N<sub>2</sub> is observed, where its width is somewhat narrower than previous observations. From the rotational distribution of N<sub>2</sub> due to photoexcitation from the (000) and (010) states of N<sub>2</sub>O and the ion image of state-selected N<sub>2</sub>, the magnitude of the transition strengths from the (000) and (010) levels were estimated. The angular anisotropy of N<sub>2</sub> fragments is in excellent agreement with the results by Neyer *et al.*<sup>2)</sup> Rather low angular anisotropy,  $\beta < 1.0$ , indicates that photoabsorption to the A''(<sup>1</sup>Σ<sup>-</sup>) state is not negligible at 205 nm.

#### References

1) Suzuki *et al.*, *Chem. Phys. Lett.* **256**, 90 (1996).

2) Neyer *et al.*, *J. Phys. Chem. A* **103**, 10388 (1999).

## III-H Development of New Devices for Molecular Dynamics Experiments

### III-H-1 Three Dimensional Photofragment Imaging Using a Fast Response Imager

SUZUKI, Toshinori; KATAYANAGI, Hideki

An inverse Abel transform is often used for reconstructing a 3D object from its 2D projection, when the original distribution is cylindrically symmetric. In pump and probe experiments, this condition is fulfilled only when the polarization directions of the two beams are aligned parallel to each other. For investigating vector correlation in photodissociation, it is useful to use cross polarization of two laser beams, which inevitably destroys the cylindrical symmetry required for an inverse Abel transform. For obtaining the 3D scattering distribution for cross polarization, time and position sensitive detection methods must be employed. Currently, a delay line anode imaging device is widely used for the time and position sensitive detection of particles. However, this method is able to receive particles only less than 10 in a given response time, about 10 ns, and it is not ideal for the experiments with low repetition lasers, where tens of particles are detected within 10 ns. We use a dual microchannel plate backed by a plastic scintillator with an emission life time of about 3 ns and capture a transient image on this screen with a gated camera with a time-resolution of 3 ns. Several designs for the acceleration electrodes were carefully tested.

### III-H-2 High Repetition Rate Two Dimensional Imaging Using C-MOS Imager

SUZUKI, Toshinori; TSUBOUCHI, Masaaki

The imaging experiment suffers from non-uniform

sensitivity of an imaging system over the area. This originates from an unavoidable pulse height (brightness) distribution of an MCP with a phosphor screen, and the most effective method to correct it is to perform real-time image processing on each image due to a single laser shot. Previously, we have performed real-time thresholding and centroiding calculations for measurements with 25 Hz system rate, while it is no longer applicable to experiments run at 1 kHz since it is by far higher rate of a regular video rate, 25 Hz. In collaboration with HAMAMATSU Co. Ltd., a 1 kHz C-MOS camera system with a real-time image processing was constructed and tested by performing 2D real-time electron counting with a 1 kHz Ti:sapphire femtosecond laser.

### III-H-3 Construction of a Rotating-Source Crossed Beam Apparatus

KOYGUCHI, Hiroshi; SUZUKI, Toshinori

A new crossed beam apparatus with a rotating source has been designed for reactive scattering experiments on the O(<sup>1</sup>D<sub>2</sub>) reactions. The crossing angle can be varied from 30 to 180 degrees for continuously changing the collision energies. The O(<sup>1</sup>D<sub>2</sub>) atoms are generated by photolysis of O<sub>2</sub> molecules at 157 nm produced by a F<sub>2</sub> laser.